Oxidation of Metals, Volume 90, Issue 5-6, 2018, pp. 555-570
DOI: 10.1007/s11085-018-9857-2

Type II Hot Corrosion Screening Tests of a Cr_2AlC MAX Phase Compound

James L. Smialek and Simon Gray
NASA Glenn Research Center, Cleveland, OH USA
Cranfield University, Cranfield, UK

Abstract

Low temperature hot corrosion tests were performed on bulk Cr_2AlC MAX phase compounds for the first time. This material is a known alumina-former with good oxidation and Type I high temperature hot corrosion resistance. Unlike traditional (Ni,Co)CrAl alumina-formers, it contains no Ni or Co that may react with Na_2SO_4 salt deposits needed to form corrosive mixed (Ni,Co)SO_4 - Na_2SO_4 eutectic salts active in Type II hot corrosion. Cr_2AlC samples coated with $20K_2SO_4$ - $80Na_2SO_4$ salt were exposed to 300 ppm SO_2 at 700°C for times up to 500 h. Weight change, recession, and cross-section microstructures identified some reactivity, but much reduced (< 1/10) compared to a Ni(Co) superalloy baseline material. Layered Al_2O_3/Cr_2O_3 scales were indicated, either separated by or intermixed with some retained salt. However, there was no conclusive indication of salt melting. Accelerated oxidation was proposed to explain the results, and coarse Cr_7C_3 impurities appeared to play a negative role. In contrast, the superalloy exhibited outer Ni(Co) oxide and inner Cr_2O_3 scales, with Cr-S layers at the interfaces. Massive spallation of the corrosion layers occurred repeatedly for the superalloy, but not at all for Cr_2AlC. This indicates some potential for Cr_2AlC as LTHC resistant coatings for superalloys.

Published by Springer. This is the Author Accepted Manuscript issued with: Creative Commons Attribution Non-Commercial License (CC:BY:NC 4.0).
The final published version (version of record) is available online at DOI:10.1007/s11085-018-9857-2. Please refer to any applicable publisher terms of use.
© This is a U.S. government work and not under copyright protection in the U.S.; foreign copyright protection may apply 2018

1) Introduction

$M_{n+1}AX_n$ "MAX Phase Compounds" have a combination of very interesting properties. Among them are high modulus, high electrical and thermal conductivity, excellent thermal shock resistance, and high damage tolerance.[1][2] Many of the properties stem from the special hexagonal crystal structure of the compounds in which 'nano-laminate' layers of MX metal carbides or nitrides are separated by layers of X (Al, Si, Ga, Ge, Sn, etc.). From the standpoint of high temperature oxidation, Al-containing MAX phases (Ti_3AlC_2, Ti_2AlC, and Cr_2AlC) have also been shown to form very protective α-Al_2O_3 scales, as summarized in a recent review [3]

Given that MAX phases have the potential for damage tolerance and the Al-MAX phases have excellent environmental resistance, they have often been proposed and studied as protective coatings for metals. Cr_2AlC has also been shown to be very resistant to Type I hot corrosion, i.e., at 900°C, or above the melting point (880°C) of typical Na_2SO_4 salt deposits in turbine engines.[4] Ti MAX phases are known to form non-protective $Na_2O{\cdot}xTiO_2$ oxides Furthermore, Cr_2AlC has a higher CTE (~13 x 10^{-6}/°C) than Ti_2AlC (8 x 10^{-6}/°C) and would present a better thermal expansion match to most Ni-base alloys (~16 x 10^{-6}/°C). For these reasons, Cr_2AlC has been proposed as a Type II, low temperature, hot corrosion (LTHC) resistant coating for superalloy disk materials.[5] The coating would preclude the formation of Ni or Co eutectic salts occurring at 660° for Ni and 585°C for Co that form under Na_2SO_4 deposits at low pO_2 and high $p(SO_3)$ conditions. [6][7][8][9]

A preliminary sputter coatings corrosion study has produced a thin 1 μm layer of Cr_2AlC on a pure Ni 201 substrate. Although testing at 700°C, under a $p(SO_2)$ of 2 ppm for 250 h, diffused the coating into the Ni surface layer, it was more resistant to oxidation under Na_2SO_4 salt deposits than Al-C, Cr-C, Al-Cr binary films or the bare substrate. [10] A diffusion bonded hybrid Cr_2AlC – superalloy couple was found to be mechanically and environmentally stable after multiple cycles and thermal exposure to 800°C for 1000 h. While little additional interdiffusion occurred at 800°C, bonding at 1100°C for 2 h had already produced appreciable 50 μm layers of NiAl and Cr_7C_3.[11] Finally, a 760°C low cycle fatigue study demonstrated no additional detriment of hot corrosion to LCF life for a Cr_2AlC-coated LSHR (low solvus, high refractory) disk superalloy.[5] Little indication of corrosive products was observed and only as occasional small platelets of $Mg(Al,Cr)_2O_4$. No corrosion pits, typically a problem for the bare superalloy, were produced in the coated samples. Agressive LCF mechanical testing did, however, produce an array of

circumferential tensile cracks in the coating, as it did even for more ductile Ni-Cr-Y coatings. Nevertheless, substrate depressions caused by excessive grit blasting were more likely than coating cracks or corrosion pits to serve as the subsequent fracture origins causing failure.

The above discussion highlights interest in the Cr_2AlC MAX phase as a Type II corrosion resistant coating for superalloys. It would therefore be useful to further characterize the LTHC behavior of this material in bulk. In that regard, three versions of Cr_2AlC and samples of the LSHR disk superalloy were exposed to a Type II hot corrosion screening process instituted at the Cranfield University. Here a $20K_2SO_4 - 80Na_2SO_4$ salt mixture was spray deposited every 50 h. Exposure to 700°C gas with 300 ppm SO_2 was performed for 500 h, with periodic inspections. Duplicate samples were pulled at various times to allow a timeline of corrosive material loss to be developed. Corrosion layers produced by 500 exposures were characterized by elemental rasters of cross sections. The purpose of this study was to obtain some more detailed chemical attack information regarding Type II hot corrosion of the Cr_2AlC MAX phase. The results are compared to an advanced disk superalloy initially examined in the hybrid diffusion couple study and the preliminary coating LCF study. Other single crystal alloys were also included in the testing, such as CMSX-4, Rene'N5, SC180, and LDS (low density) superalloys, but not reported here.

2) Experimental

Sintered ingots of a Cr_2AlC MAX phase were obtained from Kanthal/Sandvik. One (Cr_2AlC-3) was estimated to be 96% of the 5.22 g/cm^3 theoretical density of Cr_2AlC and a second (Cr_2AlC-1) was estimated to be 67%. A portion of the latter was subsequently hot pressed at 1300°C for 2 h at 35 MPa and achieved 97% density. A third high purity sample (HP) was obtained from Delft University (courtesy of Prof. W. Sloof) and was estimated to be 100% dense. A representative superalloy disk alloy, LSHR (low solvus, high refractory), was also exposed for reference: (Ni-20.4Co-12.3Cr-4.3W-3.4Ti-3.4Al-2.7Mo-1.5Ta-1.5Nb-0.05Zr-.03B-.04C). Initial SEM/EDS characterization was performed on an Hitachi S-4700 FEG-SEM. XRD diffractometer scans were obtained on the as-received material using a Bruker D8 Advance diffractometer and Cu K_α radiation.

Low temperature, Type II hot corrosion was performed on small, roughly 1 x 5 x 10 mm, rectangular samples that had been prepared to a 2400 grit finish by polishing on emery papers. A saturated aqueous salt mixture of 20 K_2SO_4 – 80 Na_2SO_4 (mole %, $T_{eutectic} \approx 823°C$) was sprayed on the samples while heated on a hot plate. Samples were weighed and one side was coat/recoated at ~ 0.5 mg/cm^2 of salt deposit for every 50 h of testing. The test was conducted at 700 °C in air charged with 300 vpm SO_2 (flow rate of 50 cm3/min). Exposures were made in a vertical alumina tube furnace using alumina hardware. Sample removal and cooling was performed every 25 h. Duplicate samples were employed and removed from test at 100, 200, 300, and 500 h to allow surface recession to be estimated by cross sectional metallography using dimensional metrology procedures. Samples were mounted in epoxy and polished with non-aqueous media to retain water soluble salts and corrosion products. Corroded samples were examined by optical photography, microscopy, and SEM/EDS elemental raster mapping. Further experimental test details can be found in prior works [Simms et al. and Sumner et al.][12] [13]

3) Results

The weight change results for four samples of as-sintered 96% dense type (A) Cr_2AlC-3 are presented in **Figure 1**. Relatively consistent gains are shown for three of the samples, with a slightly lower rate for one sample. The weight gain expected from the rate of salt deposition, assuming no vaporization or sample oxidation, is given by the dashed curve. It is seen to lie in between the measured data, which is the net sum of salt deposition added, vaporization losses, and hot corrosion / oxidation / spallation. By comparison, oxidation in air at 800°C for 1000 h produced a weight gain of only 0.1 mg/cm^2, indicating that scale growth here at 700°C would only account for a small fraction of the exhibited gain.[14] Similarly, the results for the four samples of the hot pressed 97% dense Cr_2AlC-1 type (B) material produce a tight spread distributed about the dashed line corresponding to salt deposition, **Figure 2**. Finally, the two samples of the 100% dense Cr_2AlC (Sloof/Delft) type (C) material produced weight change curves slightly below the index for salt deposition, **Figure 3**. In general, it can be stated, then, that the LTHC weight change curves follow salt deposition rates with some consistency, although the values may obscure a combination of deposition combined with slight amounts of corrosion and salt vaporization.

Fig 1. Progressive 700°C LTHC weight change of four sintered (A) Kanthal Cr_2AlC-3 samples. Little indication of excessive growth or spallation. 0.5 mg/cm^2 $20K_2SO_4$-$80Na_2SO_4$ deposited every 50 h. (Dashed line indicates approximate salt loading weight).

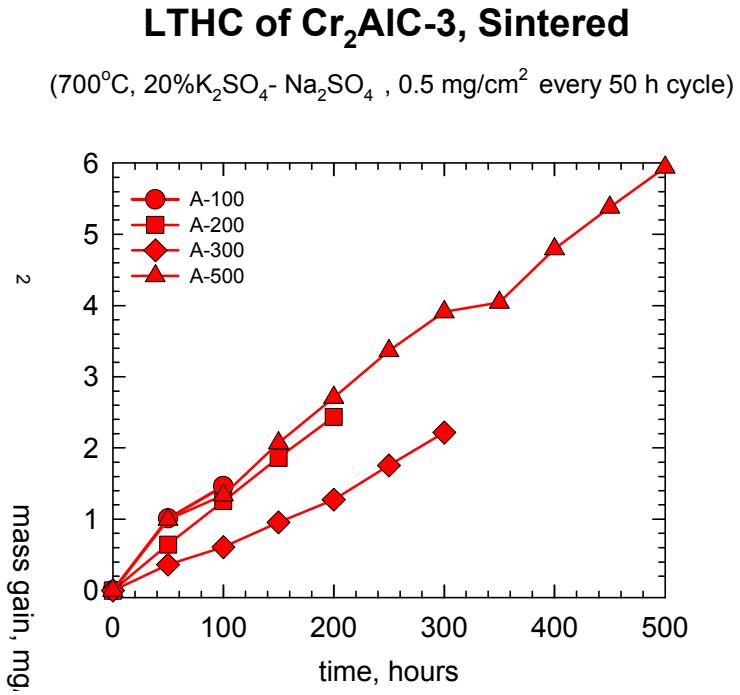

Fig 2. Progressive 700°C LTHC weight change of four hot pressed (B) Kanthal Cr_2AlC-1 samples. Little indication of excessive growth or spallation. 0.5 mg/cm^2 $20K_2SO_4$-$80Na_2SO_4$ deposited every 50 h. (Dashed line indicates approximate salt loading weight).

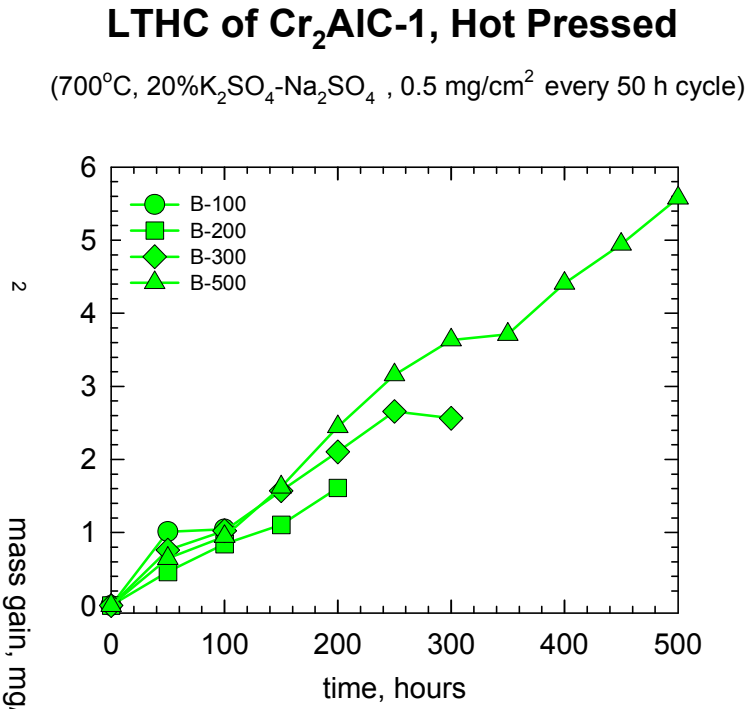

Fig 3. Progressive 700°C LTHC weight change of two 100% dense (C) Cr_2AlC (Sloof) samples. Little indication of excessive growth or spallation. 0.5 mg/cm^2 20 K_2SO_4-80Na_2SO_4 deposited every 50 h. (Dashed line indicates approximate salt loading weight).

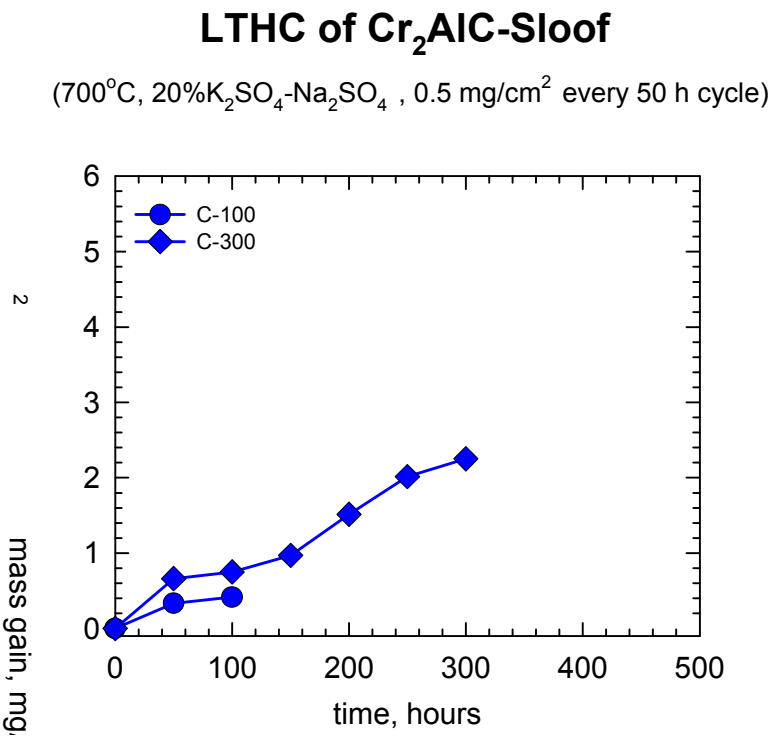

In contrast, the weight change behavior of the type (D) LSHR disk superalloy is shown in **Figure 4**. Two samples roughly follow the salt deposition rate for 100-200 h. However, the other two deviate substantially and suggest massive spallation of corrosion products, greatly exceeding the amount of salt initially added. At the end of the test, the weight loss was nearly 10 times the total weight of salt added.

Additional insights can be gained by the visual appearance of the samples. Photographs of of the four (A) Cr_2AlC-3 samples show surface modification due to salt deposition/reactions with time in **Figure 5**. A lumpy, blue or patina surface is characteristic of the coated side. The uncoated underside is clearly affected from salt contamination from the spray process or from the top surface coating. Similar results are presented for (B) Cr_2AlC-1 in **Figure 6**. The 100 h sample indicates a severe corrosion reaction at one corner. The uncoated side of the 300 h sample appears to have some long range effects of salt flow or surface diffusion, i.e., without deposit lumps.

Fig 4. Progressive 700°C LTHC weight change of four (D) LSHR disk superalloy samples. Eventual weight loss indicates repeated spallation of thick corrosion layers. 0.5 mg/cm^2 20 K_2SO_4-80Na_2SO_4 deposited every 50 h. (Dashed line indicates approximate salt loading weight).

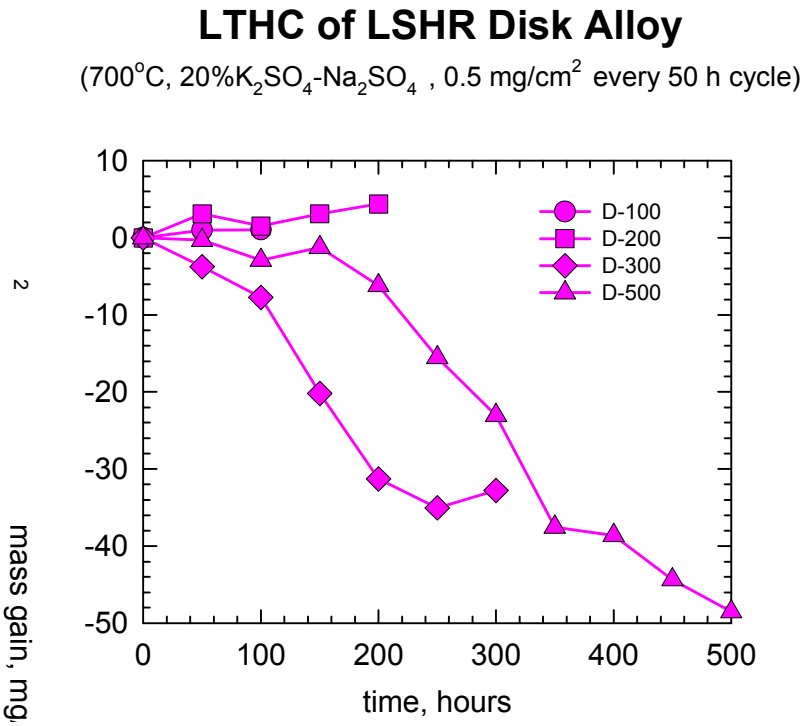

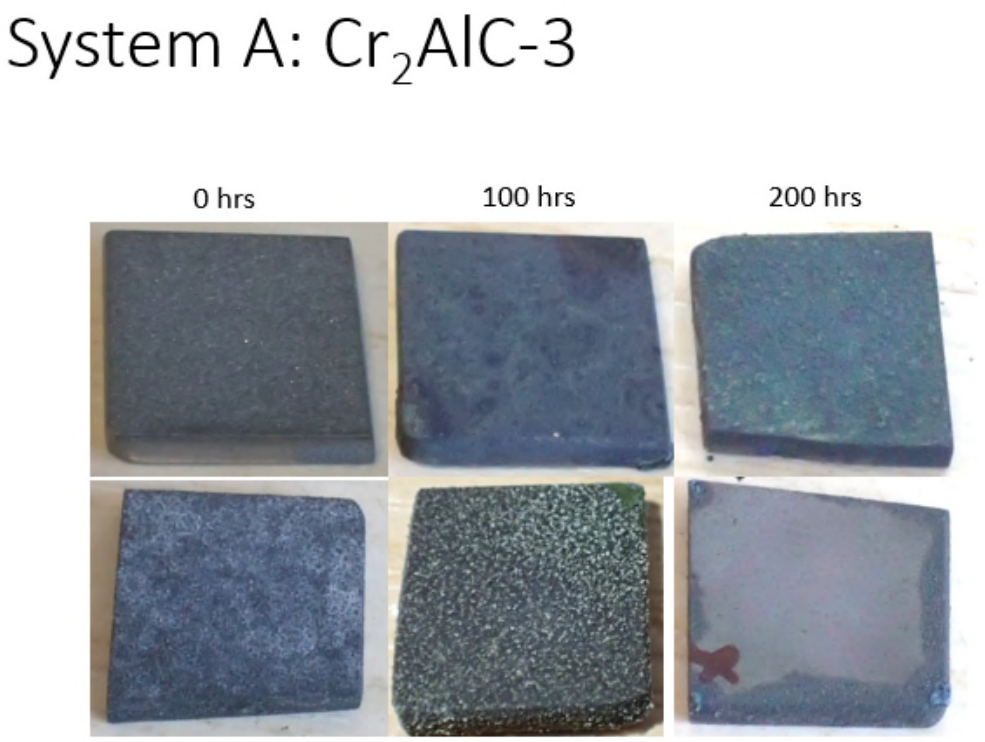

Fig 5. Surface appearance of four sintered (A) Kanthal Cr_2AlC-3 samples under 700°C LTHC. Some discoloration and corner attack of 100 h sample.

System B: Cr_2AlC-1

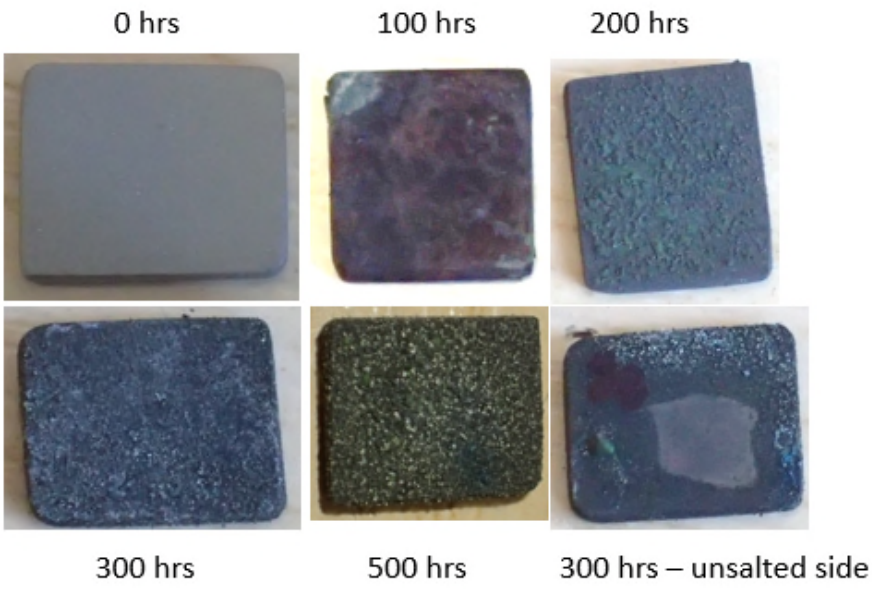

Fig 6. Surface appearance of four hot pressed (B) Kanthal Cr_2AlC-1 samples under 700°C LTHC. Some discoloration and corner attack of 100 h sample.

System C: Sloof

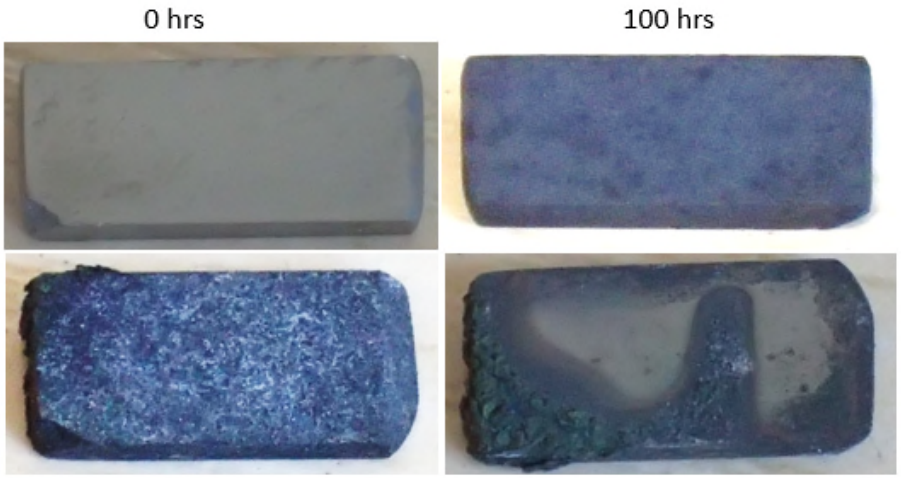

Fig 7. Surface appearance of two 100% dense (C) Cr_2AlC (Sloof) samples under 700°C LTHC. Some discoloration and corner attack of 300 h sample.

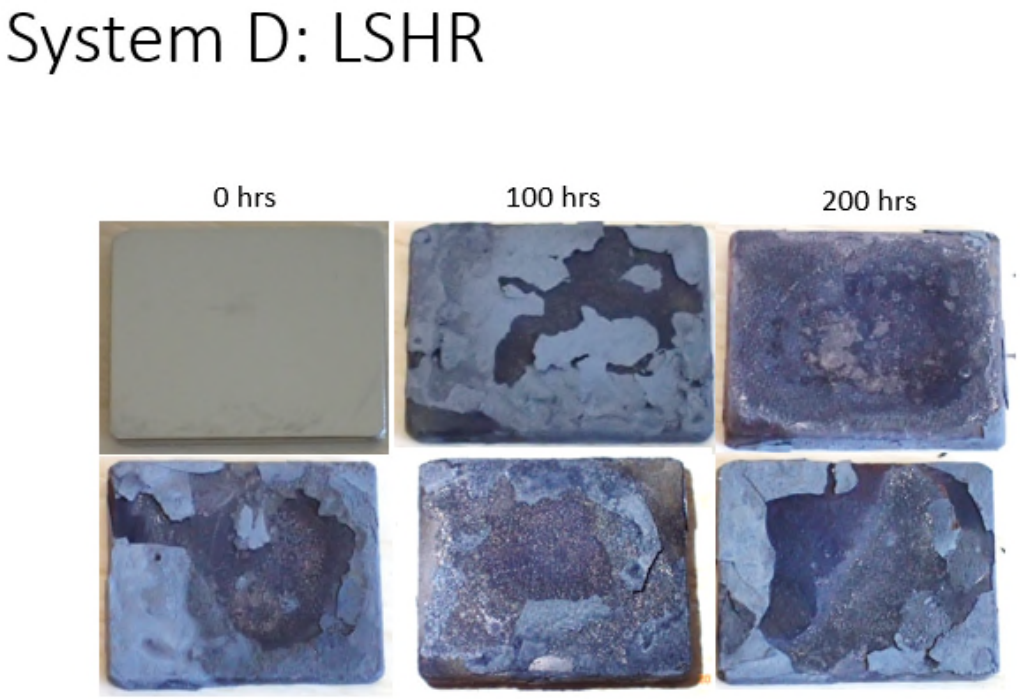

Fig 8. Surface appearance of four (D) LSHR disk superalloy samples under 700°C LTHC. Some discoloration and massive spallation layers for all samples.

Finally, the 100% dense Cr_2AlC sample exhibits a very friable surface product in **Figure 7**, with perhaps some aggressive attack at sample corners. By comparison, the exposed LSHR superalloy exhibits a great deal of non-uniformity, **Figure 8**. Large areas appear to have shed salt + corrosion layers, even quite dramatically on the uncoated bottom side.

The amount of material loss from corrosion was estimated from cross section thickness and presented in **Figure 9** along with regression fits to the data. As expected the 100% Cr_2AlC type (C) samples showed the smallest losses, with increasing amounts for the 96% and 97% dense samples, types (A) and (B). While it is no surprise that the superalloy exhibits the greatest loss, it would seem that the Cr_2AlC MAX phase samples should have been much lower. For example, the weight loss shown in **Figure 4**, at ten times the gain of the Cr_2AlC samples, is not consistent with only a 2x difference in thickness loss compared to the most severely attacked type (B) Cr_2AlC-1 samples.

Low magnification optical photomicrographs of polished cross-sections are presented in **Figure 10**. The two (A, B) Kanthal samples (500 h) exhibit a fairly continuous layer with some variation in penetration depth, or shallow pits, and retained surface nodules. The C-type Cr_2AlC material (300 h), shows some distinct corrosion pitting, with only a very thin surface scale between the pits. The LSHR alloy (500 h) exhibits an undulating, multilayer corrosion product, but with little pitting characteristics.

Chemical insights can be gained by the elemental rasters of polished cross sections. The images for type (A) Cr_2AlC, tested in LTHC conditions at 700°C for 500 h, are presented in **Figure 11** (Raster A). The SEM secondary electron image indicates a notable amount of secondary phases. The white particles represent the Cr_7C_3 second phases as they match the Al-poor dark regions in the elemental aluminum map and slightly Cr-rich regions in the Cr map. Many of the fine dark phases are seen to be bright in the aluminum map and thus correspond to the Al_2O_3 impurity phase in the substrate.

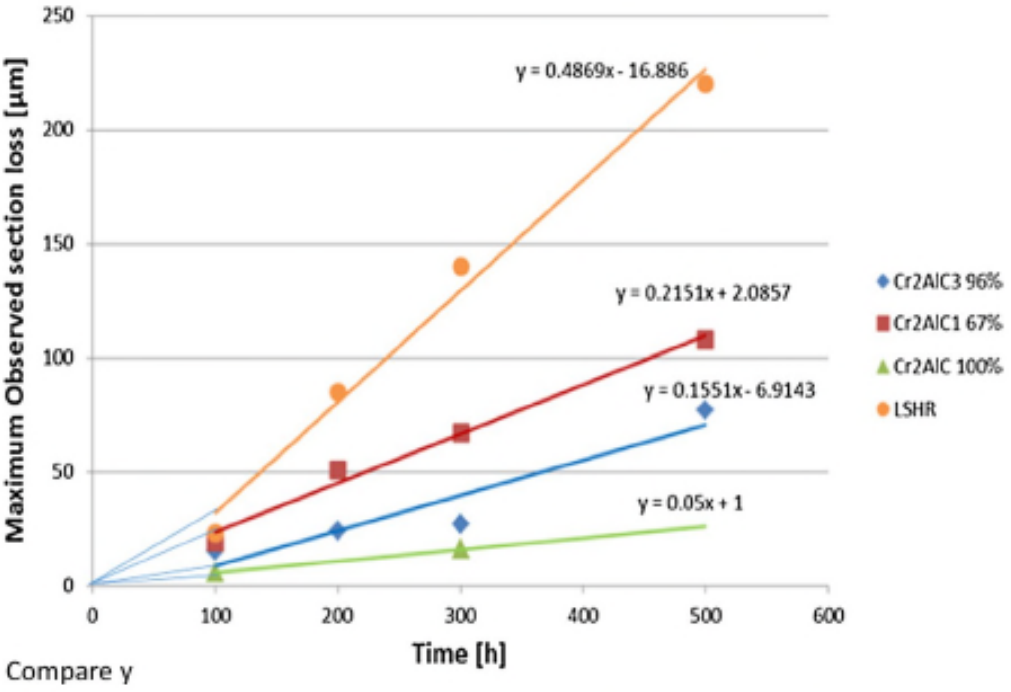

Fig 9. Surface recession loss curves representing all previous samples. The rate of attack follows (D) LSHR> (B) > (A) > (C) Cr_2AlC.

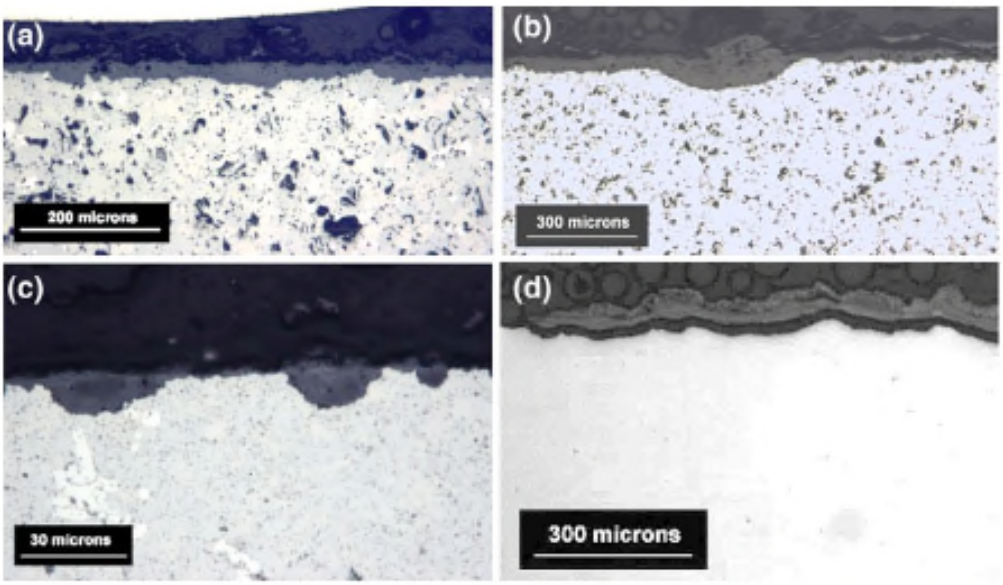

Fig 10. Optical photomicrographs of (a) sintered, (b) hot pressed Kanthal Cr_2AlC, (c) High purity Cr_2AlC (Sloof), and (d) LSHR disk superalloy after Type II hot corrosion at 700°C. (all 500 h, except 300 h for (c)).

The corrosion surface layer above the substrate shows a shallow corrosion pit, over 100 μm deep, and is primarily 'oxide' throughout as shown by the oxygen map. There appears to be a distinct demarcation boundary, approximately halfway up in the corrosion layer. This boundary is enriched in Na and S, presumably Na_2SO_4. The scale is Al-rich above this sulfate layer and Cr-rich below it. There is some suggestion that the entire oxide layer contains low levels of sulfur.

The cross section elemental raster results for the hot pressed sample (B) Cr_2AlC after 500 h hot corrosion are presented in **Figure 12** (Raster B). Again a shallow corrosion pit is shown, correlated with an outer nodule, giving a corrosion surface features more than 200 μm thick. Na and S can be seen to be more dispersed, with large regions in the nodule and smaller particles defining a line of demarcation closer to the substrate. The oxide appears Al-rich just above this line and Cr-rich just beneath it. Other regions analyzed showed similar shallow pit/external nodule features for both samples, with variations on the distribution of the sulfate phase.

The morphology and composition of the corrosion layer formed on sample (C) Cr_2AlC after 300 h hot corrosion is presented in **Figure 13a** (Raster C1). Less Cr_7C_3 (bright) and fine Al_2O_3 (dark)

ae seen in the substrate material compared to sample (A) Cr_2AlC. Also, distinctive, but small, 25 μm pits are now observed in the substrate and are associated with external nodules of about the same magnitude. While the nodules exhibit some Na + S enrichment, there is less distinctive S enrichment in the pit. No Al or Cr differentiation by layers is apparent in these elemental rasters. Another region, **13b**, (Raster C2) presents similar information. Both regions show little if any surface oxide between the pit/nodule features. (Note that K-rich areas were marginally detected and strongly correlated with Na-rich regions for all the Cr_2AlC samples).

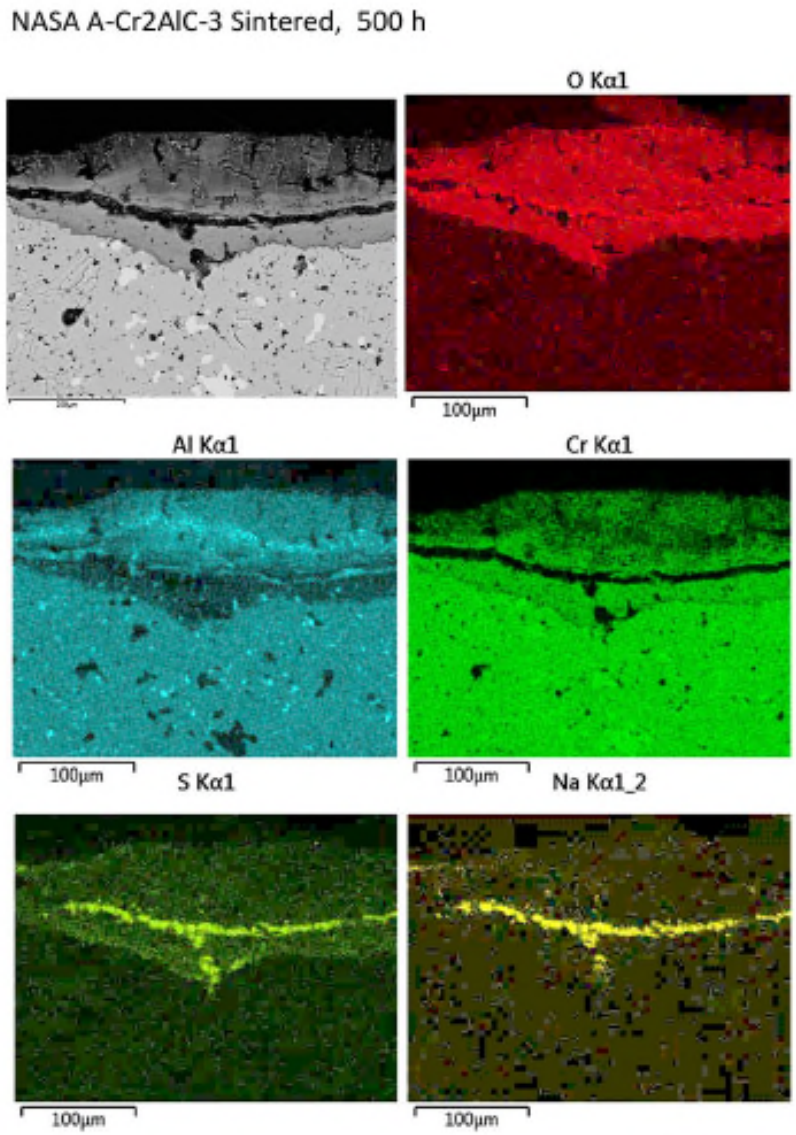

Fig 11. Elemental SEM/EDS rasters for hot corrosion tested (A) Kanthal Cr_2AlC-3 sample after 500 h at 700°C showing Al-oxide outer, Cr-oxide inner, and residual Na-S-O mid layers.

A more quantitative EDS point analysis was performed on sample (A) Cr_2AlC-3. The overall area, presented in **Figure 14a**, shows the major features of an irregular attack front, a grey matrix or substrate phase, and both light and dark dispersed impurity phases. Specific features analyzed are shown in greater detail as marked in **14b**. The results are presented in Table 1 as ZAF-corrected and normalized atomic %. The grey matrix Cr_2AlC phase is represented by spectrum #8, primarily Cr, Al, C, with some oxygen. The dark Al_2O_3 particles are represented by spectrum #7, primarily Al and oxygen, with some Cr and C. And the light Cr_7C_3 impurity phase is represented by spectrum #6, primarily Cr and C, with some Al and oxygen. These substrate analyses are in qualitative agreement with SEM/EDS studies on the same material.[11]

The central part of the scale is represented by spectrum #3, primarily Cr, Al, and oxygen, with low Na(K) and S, and appears to be $Cr(Al)_2O_3$ mixed with $Na(K)_2SO_4$. Spectrum #4 is similar, but with higher Cr and lower sulfate. The outermost layer represented by spectrum #5 has a similar make-up, but with higher Al and less oxygen.

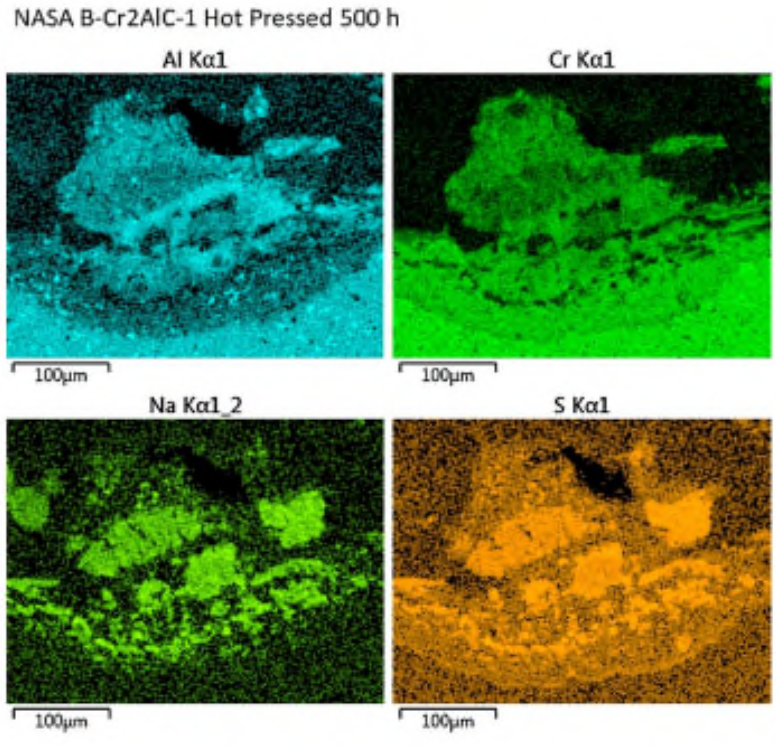

Fig 12. Elemental SEM/EDS rasters for hot corrosion tested (B) Kanthal Cr_2AlC-1 sample after 500 h at 700°C showing Al-oxide outer nodule, Cr-oxide inner layers, mixed with dispersed residual Na-S-O islands.

By contrast, the results for the LSHR disk superalloy after 500 hot corrosion are presented in **Figure 15**. Here a stratified ~ 75 μm thick external corrosion is observed. Based on the lack of Na-rich regions, it appears there is no Na_2SO_4 salt remaining. However, there are distinctively sulfur-rich regions at the metal interface and near the midplane of the scale. The outer region is heavily Ni (Co) enriched, while the inner layer is Cr-rich. A notional description of the prominent inner-to-outer layers might be Cr_2AlC-CrS-Cr_2O_3-CrS-NiO-CoO.

4) Discussion

The low temperature Type II hot corrosion resistance of Cr_2AlC MAX phase materials is reported here for the first time. The weight change behavior is not too demonstrative in that it tracks the deposit weight fairly close, with no major bifurcations indicative of runaway attack or massive spallation. However, photographs of the surface appearance suggest some level of reaction, and the uncoated backsides revealed at least a contamination color. The surface topography may primarily indicate that nodules of Na_2SO_4 formed during precipitation from the aqueous deposition solution, then sintered at 700°C. The elemental rasters do indicate some residual sulfate salt, but also show substantial thicknesses of stratified Al_2O_3/Cr_2O_3 stratified layers. The level of oxide formation greatly exceeds that expected under O_2 alone.

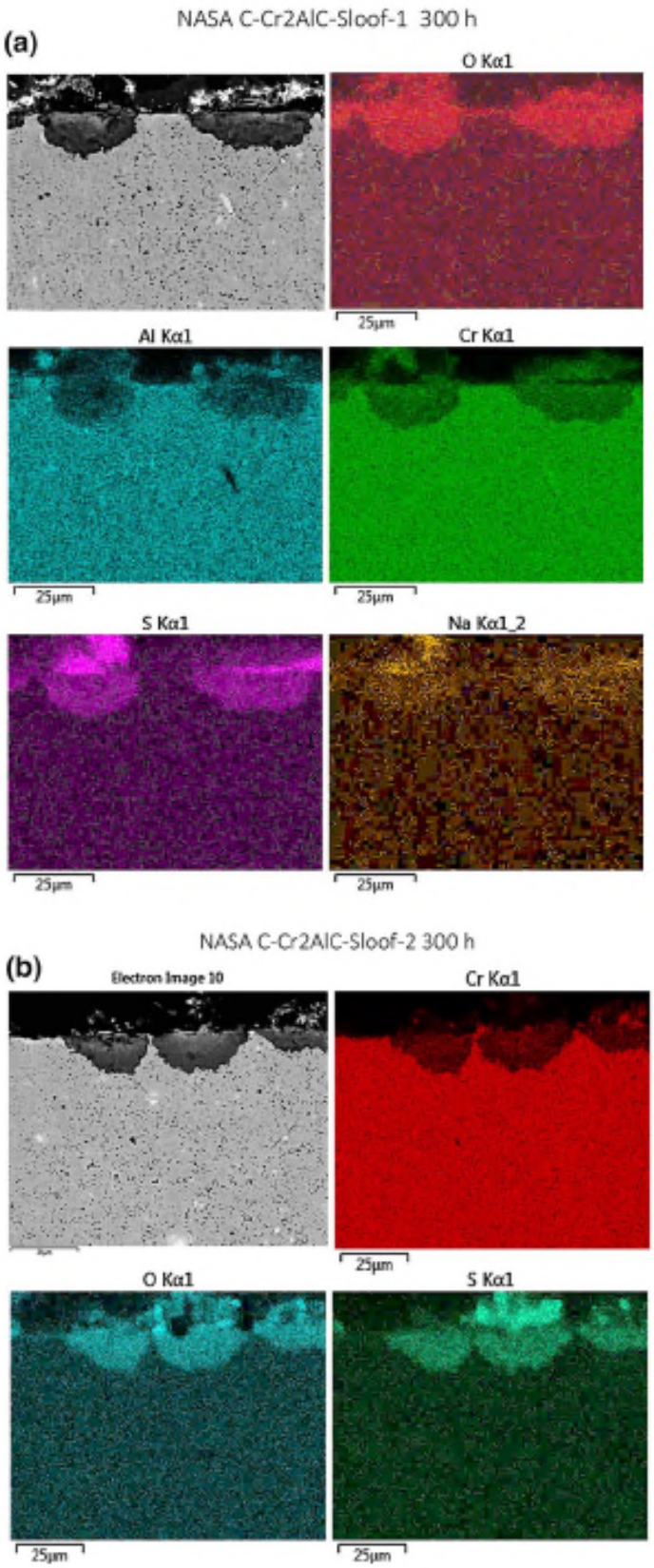

Fig 13. Elemental SEM/EDS rasters for hot corrosion tested (C) 100% dense Cr_2AlC sample after 300 h at 700°C showing Al-oxide outer nodule, Cr-oxide inner pit, both intermingled with residual Na-S-O.

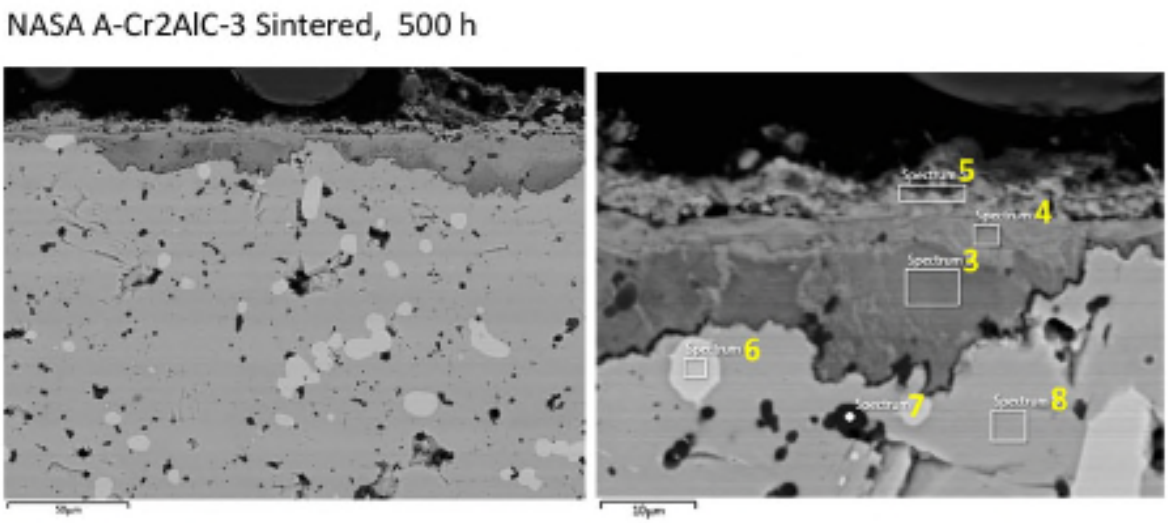

Fig 13. Elemental SEM/EDS rasters for hot corrosion tested (C) 100% dense Cr_2AlC sample after 300 h at 700°C showing Al-oxide outer nodule, Cr-oxide inner pit, both intermingled with residual Na-S-O.

Table I. Point and area EDS analyses of features in sample (A) Kanthal Cr_2AlC-3 after corrosion testing for 500 h at 700°C. #3 ,4, 5 in scale; #6, 7, 8 in Cr_2AlC substrate.

point	Cr	Al	C	O	Na	K	S	Σ	primary	secondary
3	**24.4**	6.2	0.1	**61.5**	2.7	0.7	4.4	100	$(Cr,Al)_2O_3$	$(Na,K)_2SO_4$
4	**33.5**	4.8	0.0	**59.2**	0.6	0.2	1.8	100	$(Cr,Al)_2O_3$	$(Na,K)_2SO_4$
5	35.3	12.1	0.0	49.6	1.1	0.3	1.6	100	$(Cr,Al)_2O_3$	$(Na,K)_2SO_4$
6	**62.6**	1.3	**31.1**	4.9	0.1	0.1	0.0	100	Cr_7C_3	
7	3.3	**33.0**	9.3	**54.4**	0.0	0.0	0.0	100	Al_2O_3	
8	**48.7**	**22.4**	**25.3**	3.5	0.0	0.1	0.0	100	Cr_2AlC	

K-Na sulfates do not melt below 823°C. There is no Ni or Co present to form low melting Ni(Co)-Na_2SO_4 eutectics with the substrate. According to Misra, $p(SO_3)$ greater than 10^{-2} atm. are needed for liquid $Al_2(SO_3)_4$ - Na_2SO_4 solutions to form. Typically 0.15 % SO_2 corresponds to combustion of 1% S in the fuel, yielding 10^{-3} atm. $p(SO_3)$, according to Luthra and Wood.[15] The current tests were performed at only 0.03 x10^{-2} % SO_2, and so would produce even lower $p(SO_3)$ and no

chance of liquid Al-Na sulfates. Under the present conditions, the p(SO_3) predicted by FactSage was 7.15 x 10^{-4} atm. [calculation courtesy of N. Jacobson, NASA] and well below the levels needed for liquid. Furthermore, Misra predicted only 3 ppm Cr_2O_3 would dissolve in $NiSO_4$-Na_2SO_4 melts, again only under high 10^{-2} atm. p(SO_3).[8] Thus, since eutectic dissolution mechanisms are not expected between Al-Na_2SO_4 or Cr-Na_2SO_4 at moderate p(SO_3), this suggests some unusual accelerated oxidation mechanism, ***without*** liquid salt formation, presumably due to the combined presence of C/Na/S/SO_2.

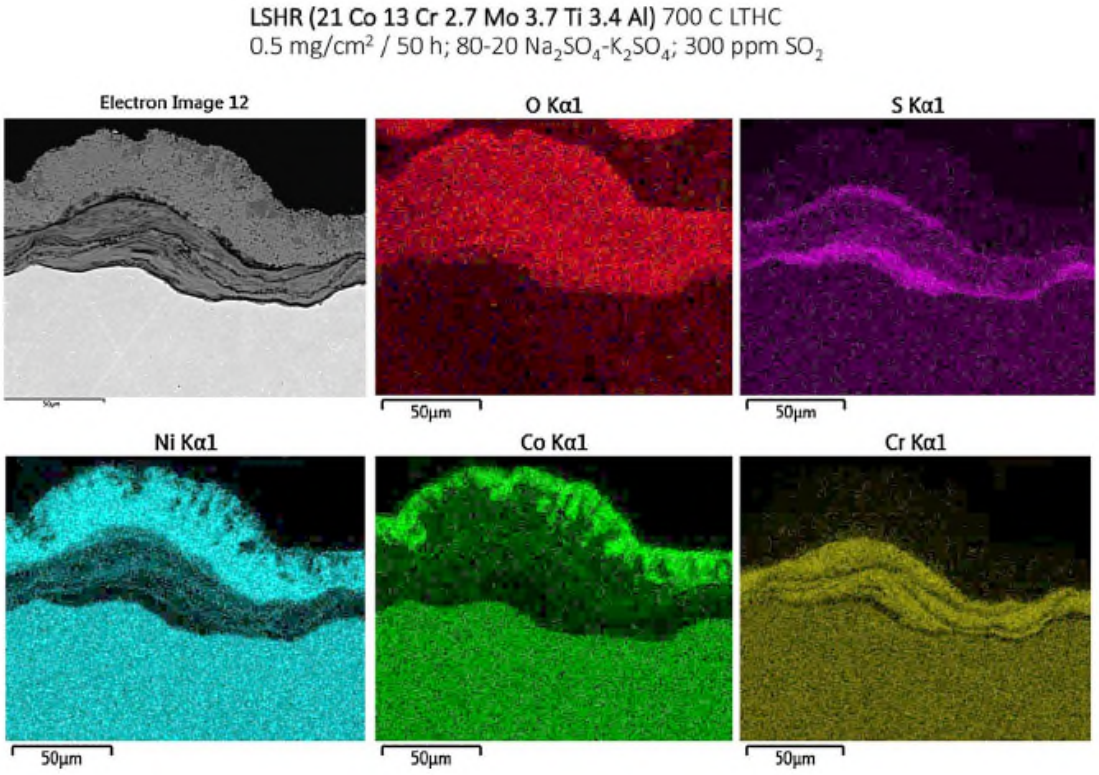

Fig 15. Elemental SEM/EDS rasters for hot corrosion tested (D) LSHR disk superalloy sample after 500 h at 700°C showing Ni(Co)-oxide outer layer, Cr-oxide inner layer, bounded by Cr-S bands. No residual Na-S-O regions.

It should be noted that all versions of the Cr_2AlC MAX phase tested here contained measurable amounts of Cr_7C_3 impurity phase which has a propensity to form a dimpled Cr_2O_3 surface scale

locally. [16] It is not known how this may affect hot corrosion. The Sloof sample did have a finer distribution of impurity phases overall and exhibited the least LTHC. Reitveld analysis yielded only 0.1 wt.% Cr_7C_3 compared to 8.9 wt. % for Type A sintered Cr_2AlC.

Hot corrosion studies of bulk Al_2O_3 revealed very little dissolution under basic or acidic conditions at 700° or 1000°C.[17] Mostly Na, Mg, Al-silicate crystals formed, and these were generally dependent on the impurity content of the ceramic. These features were generally on a fine scale and do not seem to correlate with the thick layers presented in the elemental rasters of Cr_2AlC materials tested in the present study.

By contrast, initial melting of the salt is expected for Ni(Co) superalloys. Eutectic temperatures of $NiSO_4$-Na_2SO_4 and $CoSO_4$-Na_2SO_4 mixes are only 660° and 585°C, respectively. Furthermore, the equilibrium $p(SO_3)$ for liquid $CoSO_4$-Na_2SO_4 salt compounds vs solid CoO is only 4 x 10^{-6} atm. at 700°C, or well below the 10^{-3} atm. calculated for the 0.15% SO_2 example (Luthra and Wood).[15] Given the existence of molten salts, classic accelerated hot corrosion by Ni(Co)O scale dissolution and re-precipitation at the higher $p(O_2)$ outer regions of the reaction layer are expected. At the lowest $p(O_2)$ inner regions, CrS may be formed, as suggested by the stability diagram for LTHC.[7] This is exactly what is seen in **Figure 15**. Presumably, S was removed from Na_2SO_4, while Na_2O was lost by vaporization. Subsequent oxidation converts CrS to Cr_2O_3. (Misra)[18] What is not apparent in cross section is the extent of corrosion suggested by the excessive final weight loss near 50 mg/cm^2. Indeed, the scale thickness was only about 100 µm thick. Repeated spallation on cooling apparently shaves off thick outer layers, as indicated by the photos, and recoating with salt resumes the corrosive attack.

Lastly, pitting corrosion was not a distinctive feature here, as is often called out in Type II LTHC mechanisms. This is consistent with other studies, where higher SO_2 pressures result in aggressive uniform corrosion rather than just at the limited regions of pitting. Pits are more typical for very low 10 ppm SO_2 pressures.[19] It should also be noted that limited 700°C testing of Type B hot pressed Cr_2AlC exhibited 40Mg_2SO_4 -60Na_2SO_4 corrosion and pitting under 0.1% SO_2, but no attack under 0.005% (50 ppm) SO_2, even though the salt was liquid at about 660°C [unpublished research by J. Nesbitt, J. Smialek, NASA].

5) Conclusions

Type II low temperature hot corrosion of bulk Cr_2AlC was examined for the first time under aggressive conditions. As-expected, there was little evidence that a molten sulfate eutectic formed. However, some type of accelerated attack indeed took place. The severity was not necessarily exhibited by the progressive weight gain curves, which showed no real anomalies. But rather it was exhibited in the significant thickness (recession) losses of 25-125 μm measured in cross sections. This correlated with mixed layers of Al_2O_3-Na_2SO_4-Cr_2O_3 that exceeded normal oxidation rates, approaching 100 μm in the thicker regions. The least reaction was exhibited by the material with the lowest amount of Cr_7C_3 second phase and the finest microstructure. Less severe tests under 50 ppm SO_2 are expected to show little attack, while superalloys are still susceptible to LTHC pitting. The potential for Cr_2AlC as protective LTHC resistant coatings is therefore reasonable provided the purity and microstructure can be refined.

References

[1] M. W. Barsoum and T. El-raghy, "The MAX Phases : Unique New Carbide and Nitride Materials," *Am. Sci.*, vol. 89, no. July-August, pp. 334–343, 2001.

[2] M. Barsoum *et al.*, "Thermal and electrical properties of Nb_2AlC, $(Ti,Nb)_2AlC$ and Ti_2AlC," *Metall. Mater. Trans. A*, vol. 33, no. 9, pp. 2775–2779, 2002.

[3] D. J. Tallman, B. Anasori, and M. W. Barsoum, "A Critical Review of the Oxidation of Ti2AlC, Ti3 AlC2 and Cr2AlC in Air," *Mater. Res. Lett.*, vol. 1, no. 3, pp. 115–125, 2013.

[4] Z. J. Lin, M. S. Li, J. Y. Wang, and Y. C. Zhou, "High-temperature oxidation and hot corrosion of Cr2AlC," *Acta Mater.*, vol. 55, no. 18, pp. 6182–6191, Oct. 2007.

[5] J. L. Smialek, J. A. Nesbitt, T. P. Gabb, A. Garg, and R. A. Miller, "Hot corrosion and low cycle fatigue of a Cr2AlC-coated superalloy," *Mater. Sci. Eng. A*, vol. 711, 2018.

[6] F. Pettit, "Hot corrosion of metals and alloys," *Oxidation of Metals*, vol. 76, no. 1–2. pp. 1–21, 2011.

[7] K. L. Luthra, "Low Temperature Hot Corrosion of Cobalt-Base Alloys: Part II. Reaction Mechanism," *Metall. Trans.*, vol. 13A, no. October, pp. 1853–1864, 1982.

[8] A. K. Misra, "HOT CORROSION OF NICKEL AND COBALT BASE ALLOYS AT INTERMEDIATE TEMPERATURES.," *Key Eng. Mater.*, vol. 20–28, no. pt 1-4, 1987.

[9] M. Zahiri Azar, T. Gheno, B. Gleeson, and A. H. Heuer, "Initial Stages of Na2SO4-Induced Degradation of β-Ni36Al at 700 °C: I-Intrinsic Behavior," *Oxid. Met.*, 2017.

[10] L. M. Aw *et al.*, "Investigation of Na2SO4 Deposit Induced Corrosion of Cr, Al, C Binary and Ternary Thin Film Coatings on Ni-201," *J. Electrochem. Soc. 2017 164(6)*, vol. 164, no. 6, pp. C218–C223, 2017.

[11] J. L. Smialek and A. Garg, "Interfacial reactions of a MAX phase/superalloy hybrid," *Surf. Interface Anal.*, vol. 47, no. 8, pp. 844–853, 2015.

[12] Authors: and J. E. O. N.J. Simms, John R. Nicholls, "Materials for Solid Fuel Fired Gas Turbines: Burner Rig and Laboratory Studies High Temperature Corrosion and Protection of Materials 5; Edited by: R. Streiff, I.G. Wright, R.C. Krutenat, M. Caillet and A. Galerie DOI: https://doi.org/10.4028/www.scientifi," *Mater. Sci. Forum*, vol. Volumes 36, pp. 833–840, 2001.

[13] J. Sumner, Q. Aksoul, J. Delgado, A. Potter, and S. Gray, "Impact of Deposit Recoat Cycle Length on Hot Corrosion of CMSX-4," *Oxid. Met.*, vol. 87, no. 5–6, pp. 767–778, 2017.

[14] J. L. Smialek and A. Garg, "Interfacial reactions of a MAX phase/superalloy hybrid," *Surf. Interface Anal.*, vol. 47, no. 8, 2015.

[15] K. L. Luthra and J. H. Wood, "High chromium cobalt-base coatings for low temperature hot corrosion," *Thin Solid Films*, vol. 119, no. 3, pp. 271–280, 1984.

[16] J. L. Smialek and A. Garg, "Microstructure and Oxidation of a MAX Phase / Superalloy Hybrid Interface," *NASA TM 2014-216679*, no. July, pp. 1–19, 2014.

[17] M. G. Lawson, F. S. Pettit, and J. R. Blachere, "Hot corrosion of alumina," *J. Mater. Res.*, vol. 8, no. 8, pp. 1964–1971, 1993.

[18] A. K. Misra, "Corrosion of metals and alloys in sulfate melts at 750 °C," *Oxid. Met.*, vol. 25, no. 5–6, pp. 373–396, 1986.

[19] T. Gabb *et al.*, "Cyclic Oxidation and Hot Corrosion of NiCrY-Coated Disk Superalloy," *NASA TM 2016-219105*, no. June, pp. 1–22, 2016.